

# Energetic Approach to the Folding of $\alpha/\beta$ Barrels

Kuo-Chen Chou and Louis Carlacci

Computational Chemistry, Upjohn Research Laboratories, Kalamazoo, Michigan 49001

**ABSTRACT** The folding of a polypeptide into a parallel  $(\alpha/\beta)_8$  barrel (which is also called a circularly permuted  $\beta_8\alpha_8$  barrel) has been investigated in terms of energy minimization. According to the arrangement of hydrogen bonds between two neighboring  $\beta$ -strands of the central barrel therein, such an  $\alpha/\beta$  barrel structure can be folded into six different types: (1) left-tilted, left-handed crossover; (2) left-tilted, right-handed crossover; (3) nontilted, left-handed crossover; (4) nontilted, right-handed crossover; (5) right-tilted, left-handed crossover; and (6) right-tilted, right-handed crossover. Here "tilt" refers to the orientational relation of the  $\beta$ -strands to the axis of the central  $\beta$ -barrel, and "crossover" to the  $\beta\alpha\beta$  folding connection feature of the parallel  $\beta$ -barrel. It has been found that the right-tilted, right-handed crossover  $\alpha/\beta$  barrel possesses much lower energy than the other five types of  $\alpha/\beta$  barrels, elucidating why the observed  $\alpha/\beta$  barrels in proteins always assume the form of right tilt and right-handed crossover connection. As observed, the  $\beta$ -strands in the energy-minimized right-tilted, right-handed crossover  $(\alpha/\beta)_8$ -barrel are of strong right-handed twist. The value of root-mean-square fits also indicates that the central barrel contained in the lowest energy  $(\alpha/\beta)_8$  structure thus found coincides very well with the observed 8-stranded parallel  $\beta$ -barrel in triose phosphate isomerase (TIM). Furthermore, an energetic analysis has been made demonstrating why the right-tilt, right-handed crossover barrel is the most stable structure. Our calculations and analysis support the principle that it is possible to account for the main features of frequently occurring folding patterns in proteins by means of conformational energy calculations even for very complicated structures such as  $(\alpha/\beta)_8$  barrels.

**Key words:** staggering hydrogen bonds, tilt, twist,  $\beta\alpha\beta$  crossover connection, random generation of initial structures, energy minimization, associated loop energy

## INTRODUCTION

From the aesthetical point of view, the  $\alpha/\beta$  barrel structure is probably one of the most striking struc-

tures in proteins. Such a beautiful structure is constructed as if by successively folding a chain, alternating between  $\beta$ -strands and  $\alpha$ -helices, into a cylindrical topology suggesting the general shape of a barrel. Triose phosphate isomerase (TIM) was the first example of a protein found to have this type of structure.<sup>1,2</sup> So far these structures are known to occur in 17 enzymes,<sup>3</sup> all with little sequence homology, but significant structural similarity,<sup>3,4</sup> i.e., all with 8 parallel  $\beta$ -strands as an "inner core" surrounded by 7 or 8  $\alpha$ -helices as an "outer concentric cylinder." Each inner  $\beta$ -strand is connected to an outer  $\alpha$ -helix in a right-handed  $\beta\alpha\beta$  crossover manner,<sup>5,6</sup> so to a first approximation the enzyme can be expressed as an  $(\alpha/\beta)_8$  structure.<sup>3</sup> Although this structure motif is termed a barrel, the cross section of the barrel is usually elliptical rather than circular.<sup>3</sup> Rather than being parallel to the central axis of the  $\beta$ -barrel, both the inner  $\beta$ -strands and the outer  $\alpha$ -helices are tilted so as to follow a right-handed spiral around the central axis of the barrel,<sup>7–10</sup> as reflected by having a positive shear number introduced by McLachlan.<sup>9</sup> An  $\alpha/\beta$  barrel structure with such features in tilt and crossover connection is called the *right-tilted, right-handed crossover*  $\alpha/\beta$ -barrel, as will be further described later. The topology of  $\alpha/\beta$  barrels is almost invariant, with each connection moving over by one strand and always in the same direction (right-handed as referred to the strand direction), which is why they are called singly wound barrels.<sup>11</sup> As pointed out recently by Farber and Petsko,<sup>3</sup> of the enzymes whose structure is known, roughly 1 of 10 has this kind of  $\alpha/\beta$  domain, indicating the importance of understanding this type of structure.

The existence of such a set of similar structures, arising from proteins with very dissimilar sequences, poses such a questions: why are the folds so similar? Lasters et al.<sup>12,13</sup> used a geometric model and the requirements of close packing to demonstrate that the 8-fold parallel barrel was one of only

Received May 11, 1990; revision accepted September 12, 1990.

Address reprint requests to Dr. Kuo-Chen Chou, Department of Computational Chemistry, Upjohn Research Laboratories, 301 Henrietta Street, Kalamazoo, MI 49001.

Dr. Carlacci was a postdoctoral fellow in Upjohn Laboratories from July 1, 1988 to October 15, 1990. His current address is: Department of Biochemistry & Biophysics, School of Medicine, University of Pennsylvania, Philadelphia, PA 19104-6059.

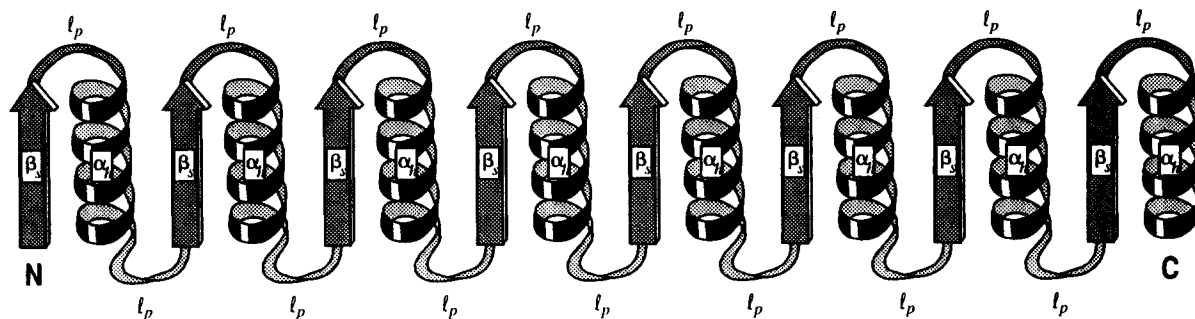


Fig. 1. Schematic illustration of a polypeptide chain in which  $\beta_s$  represents a  $\beta$ -strand and  $\alpha_h$  represents  $\alpha$ -helices. Between the adjacent  $\beta_s$  and  $\alpha_h$  segments along the chain there is a link  $\ell_p$ , which will become a loop after the polypeptide chain is

folded into an  $\alpha/\beta$  barrel. The number of  $\beta_s$  segments and the number of  $\alpha_h$  segments are the same, both equal to  $n_b = 8$ , and the number of  $\ell_p$  segments is  $(2n_b - 1) = 15$ .

a few viable barrel conformations. Lesk et al.<sup>2</sup> analyzed the packing of the residues in the interior of  $\alpha/\beta$  barrels, and found that not all proteins with this fold are related by evolution, but that they represent a common favorable solution to the structural problems involved in the creation of a closed  $\beta$ -barrel. Recently, de novo design of an  $\alpha/\beta$  barrel protein has also been engineered by Luger et al.<sup>14</sup> and Goraj et al.<sup>15</sup> in order to address this issue. On the other hand, based on structural and chemical evidence, it was proposed by Farber and Petsko<sup>3</sup> that all of these  $\alpha/\beta$  barrel domains may have diverged from a common ancestor. To the best of our knowledge, however, so far no quantitative analysis has been reported on the energetic features of such a folding motif.

The present study was initiated in an attempt to quantitatively address the issue from an energetic point of view. Our discussions were focused on the following points: What is the major factor that stabilizes the right-tilted, right-handed crossover  $\alpha/\beta$  barrel? What role do the  $\alpha$ -helix segments play? What role do the  $\beta$ -strand segments play? What role do the loop segments, which sequentially connect the  $\alpha$ -helices and  $\beta$ -strands along the chain folded into the  $\alpha/\beta$  structure, play? What role do the interactions among these three components play? Can an  $\alpha/\beta$  barrel with other handed features be folded as a stable structure?

### CLASSIFICATION OF $\alpha/\beta$ BARRELS

Let us consider a polypeptide chain (Fig. 1) in which there are  $n_b$   $\beta$ -strands ( $\beta_s$ ) and  $n_b$   $\alpha$ -helices ( $\alpha_h$ ). Between the adjacent  $\beta$ -strand and  $\alpha$ -helix along the chain there is a link ( $\ell_p$ ), which will become a loop after the polypeptide chain is folded into an  $\alpha/\beta$  barrel. The number of  $\ell_p$  segments in the polypeptide chain is  $2n_b - 1$ .

According to the tiltedness of the central  $\beta$ -barrel<sup>16,17</sup> and the chirality of the  $\beta\alpha\beta$  crossover connection,<sup>5,6</sup> such a polypeptide chain can be folded

into the following six different types of  $\alpha/\beta$  barrel structures:

1. Left-tilted, left-handed crossover  $\alpha/\beta$  barrel, as symbolized by  $B_{ll}$ .
2. Left-tilted, right-handed crossover  $\alpha/\beta$  barrel, as symbolized by  $B_{lr}$ .
3. Nontilted, left-handed crossover  $\alpha/\beta$  barrel, as symbolized by  $B_{nl}$ .
4. Nontilted, right-handed crossover  $\alpha/\beta$  barrel, as symbolized by  $B_{nr}$ .
5. Right-tilted, left-handed crossover  $\alpha/\beta$  barrel, as symbolized by  $B_{rl}$ .
6. Right-tilted, right-handed crossover  $\alpha/\beta$  barrel, as symbolized by  $B_{rr}$ .

In order to find out from an energetic point of view why all the observed  $\alpha/\beta$  barrels in proteins are of right tilt and right-handed crossover connection, it is necessary, as a first step, to establish a technique by which any of the six types of  $\alpha/\beta$  barrels can be generated as desired.

### GENERATION OF $\alpha/\beta$ BARRELS

Because so far all the  $\alpha/\beta$  barrels observed in proteins, except muconate lactonizing enzyme and mandelate racemase in which the last helix is missed, are formed by 8 strands and 8 helices as symbolized by an  $(\alpha/\beta)_8$  barrel, let us assign  $n_b = 8$ . Only L-type amino acids, the natural amino acids, were used in the current study. Without loss of generality, the amino acid sequences for  $\alpha_h$ ,  $\ell_p$ , and  $\beta_s$  segments in Figure 1 can be further assigned as follows:

$$\begin{cases} (\text{Ala})_{12}, & \text{for } \alpha_h \text{ segment} \\ (\text{Ala})_4, & \text{for } \ell_p \text{ segment} \end{cases} \quad (1)$$

$$\begin{cases} (\text{Val-Gly})_3, & \text{for the 1st, 3rd, 5th, 7th } \beta_s \text{ segments} \\ & \text{of the nontilted barrel} \\ (\text{Gly-Val})_3, & \text{for the 2nd, 4th, 6th, 8th } \beta_s \text{ segments} \\ & \text{of the nontilted barrel} \\ (\text{Val-Gly})_3, & \text{for all } \beta_s \text{ segments of the right- and} \\ & \text{left-tilted barrels} \end{cases} \quad (2)$$

The choices of amino acid sequences for  $\alpha_h$  and  $\ell_p$  and their lengths are the same as in the previous paper.<sup>6</sup> Although the length of the  $\ell_p$ - $\alpha_h$ - $\ell_p$  segment is somewhat arbitrary, it must be longer than the distance for a crossover connection between two neighboring  $\beta$ -strands. The choice of amino acid sequence for  $\beta_s$  segments ( $\beta$ -strands) as given by Eq. (2) will ensure that nearest-neighbor residues in adjacent strands are alternately Val and Gly in all of the barrels, i.e., nowhere do two large side chains occur in neighboring positions, in order to avoid large repulsive overlaps.<sup>17</sup> Valine was chosen because it is the most frequently occurring residue in  $\beta$ -strands.<sup>18,19</sup> On the other hand, space limitations inside the barrel are satisfied if there is an alternation of bulky residues (Val) and residues with small or no side chain (preferably Gly) in neighboring positions on adjacent strands. Such a pattern is seen frequently in  $\beta$ -barrels of globular proteins, and hence was adopted in the present study. The whole polypeptide chain was blocked with end groups H- and -OH at its N- and C-termini, respectively.

The procedures to generate various types of  $\alpha/\beta$  barrels are as follows.

### Build Up the Core of the Central $\beta$ -Barrel

By means of the method given by Chou et al.,<sup>16</sup> the left-tilted (Fig. 2), nontilted (Fig. 3), and right-tilted (Fig. 4) idealized parallel  $\beta$ -barrels were built up, respectively. All these barrels contain 8 strands whose amino acid sequences are given in Eq. (2). There are five idealized H-bonds between two adjacent strands for each of these three types of  $\beta$ -barrels, and their H-bond patterns are given in ref. 16. According to the spatial positions of the strands, each of these three types of barrels can be further classified into two subtypes: (1) counterclockwise type (See Figs. 2a-4a) and (2) clockwise type (See Figs. 2b-4b), i.e., if viewed along the direction of the axis Z of a parallel  $\beta$ -barrel,<sup>16</sup> the strands in the former follow a counterclockwise arrangement while the strands in the latter follow a clockwise arrangement (see the legend to Fig. 2 for further explanation). A counterclockwise parallel  $\beta$ -barrel can be used to form a left-handed crossover  $\alpha/\beta$  barrel, and a clockwise parallel  $\beta$ -barrel can be used to form a right-handed crossover  $\alpha/\beta$  barrel.<sup>11</sup>

### Connect Two Neighboring $\beta$ -Strands With an $\alpha$ -Helix

For each of these  $\beta$ -barrels thus generated, all two adjacent strands were connected with a segment  $\ell_p$ - $\alpha_h$ - $\ell_p$  (Fig. 1), whose amino acid sequences are given in Eq. (1). After all these connecting operations were done, however, the segment  $\ell_p$  between the last helix and the first strand should be cut off to make the whole  $(\alpha/\beta)_8$  barrel structure folded as if from an open chain rather than a closed chain. The process of

connecting two rigidly fixed structures ( $\beta_s$ ) with a flexible polypeptide link actually corresponds to a process of geometrical optimization, whose details have been described in the previous papers.<sup>6,20,21</sup> The starting dihedral angles of  $\alpha_h$  were those of the computed minimum-energy conformation of an isolated poly(Ala)  $\alpha$ -helix,<sup>22</sup> viz.  $(\phi, \psi, \omega, \chi^1) = (-68.1^\circ, -38.3^\circ, 180.0^\circ, 60.0^\circ)$ . The initial position and orientation of the segment  $\alpha_h$  were specified, relative to the  $\beta$ -sheet defined by the two connected strands ( $\beta_s$ ), by six external variables, viz. three Euler angles  $\bar{\alpha}, \beta, \gamma$ , and three components  $t_u, t_v, t_w$  of a translational vector.<sup>23</sup> The helix segment  $\alpha_h$  was initially oriented antiparallel to the two  $\beta$ -strands, and it was placed at the outside of the barrel, 11 Å away from the sheet concerned. Therefore, the initial position and orientation of the segment  $\alpha_h$  were defined by Euler angles  $(\bar{\alpha}, \beta) = (0^\circ, 180^\circ)$  and translations  $(t_u, t_v, t_w) = (0.0, 11.0, 0.0)$  Å and  $(0.0, -11.0, 0.0)$  Å for the cases of counterclockwise and clockwise barrels (corresponding to left-handed and right-handed  $\beta\alpha\beta$  crossover connections), respectively. Once assigned, all these values were fixed during geometric optimization. Only  $\gamma$  and the dihedral angles of the two  $\ell_p$  segments, which are attached to the two ends of the segment  $\alpha_h$ , were allowed to vary. Therefore, the central part,  $\alpha_h$ , of the link segment can be compared with a rigid rod whose only allowable motion is the rotation about its own axis and whose two ends are attached by two flexible "arms"  $\ell_p$ s.

The initial Euler angle  $\gamma$  that describes rotation of  $\alpha_h$  about its own axis and the initial dihedral angles of the two flexible links  $\ell_p$ s attached to the two ends of  $\alpha_h$  can be chosen arbitrarily, because they will be determined subsequently by the geometric optimization procedure.<sup>6</sup> In these calculations, the initial dihedral angles assigned for the two flexible "arms"  $\ell_p$ s were  $(\phi, \psi, \omega, \chi^1) = (140.0^\circ, 137.2^\circ, 180.0^\circ, 60.0^\circ)$ . A random number generator was applied to assign 100 different initial values for the Euler angle  $\gamma$ , yielding 100 different connected conformations for each type of  $(\alpha/\beta)_8$  barrel.

### Screening Procedure

For each set of 100  $(\alpha/\beta)_8$  barrels generated via the above two steps, a screening procedure was adopted to sift out 10 "candidates" as starting structures for energy minimizations according to the following criteria: (1) the candidate must be a good  $(\alpha/\beta)_8$  barrel in the geometric sense, i.e., the objective function<sup>6</sup>  $F_0$  of the geometrical fit for each  $\beta\alpha\beta$  connection must be smaller than  $0.0025 \text{ Å}^2$ , and (2) its conformational energy is one of the 10 lowest among the geometrically good  $(\alpha/\beta)_8$  barrels that satisfy criterion (1).

Thus, through the above procedure, there were  $6 \times 10 = 60$  starting conformations: 10 for each of the six different types of  $(\alpha/\beta)_8$  structures. Among the 10

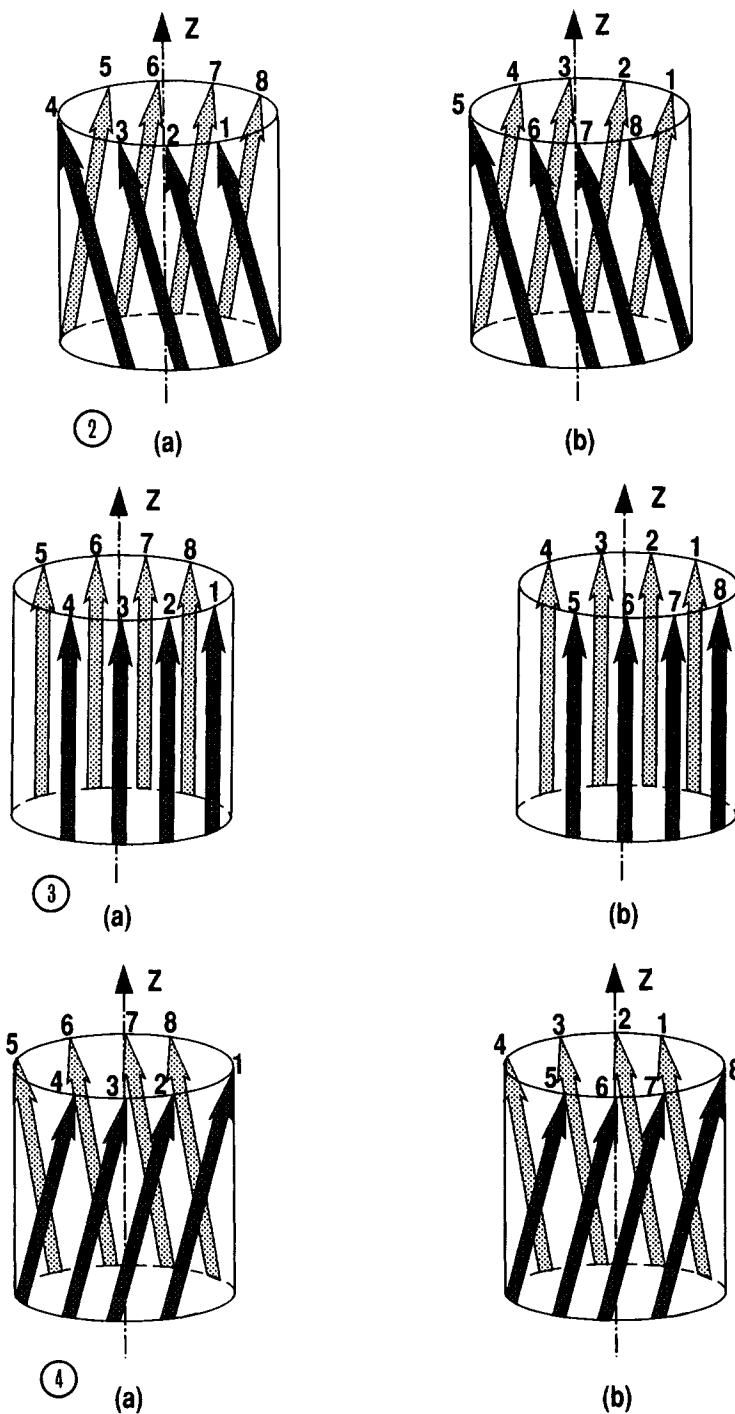


Fig. 2. Schematic illustration of a left-tilted 8-stranded parallel  $\beta$ -barrel. The strands are numbered from 1 to 8 according to the sequential order of the strands. Viewed along the direction of its axis<sup>16</sup> Z, the 8  $\beta$ -strands follow, in increasing order of number, (a) counterclockwise arrangement, and (b) clockwise arrangement. The counterclockwise left-tilted parallel  $\beta$ -barrel can be used to form a left-tilted, left-handed crossover  $\alpha/\beta$  barrel. The clockwise left-tilted parallel  $\beta$ -barrel can be used to form a left-tilted, right-handed crossover  $\alpha/\beta$  barrel.

Fig. 3. Schematic illustration of a nontilted 8-stranded parallel  $\beta$ -barrel: (a) counterclockwise arrangement, and (b) clockwise arrangement. The counterclockwise nontilted parallel  $\beta$ -barrel can

be used to form a nontilted, left-handed crossover  $\alpha/\beta$  barrel. The clockwise nontilted parallel  $\beta$ -barrel can be used to form a nontilted, right-handed crossover  $\alpha/\beta$  barrel. See the legend to Figure 2 for further explanation.

Fig. 4. Schematic illustration of a right-tilted 8-stranded parallel  $\beta$ -barrel: (a) counterclockwise arrangement, and (b) clockwise arrangement. The counterclockwise right-tilted parallel  $\beta$ -barrel can be used to form a right-tilted, left-handed crossover  $\alpha/\beta$  barrel. The clockwise right-tilted parallel  $\beta$ -barrel can be used to form a right-tilted, right-handed crossover  $\alpha/\beta$  barrel. See the legend to Figure 2 for further explanation.

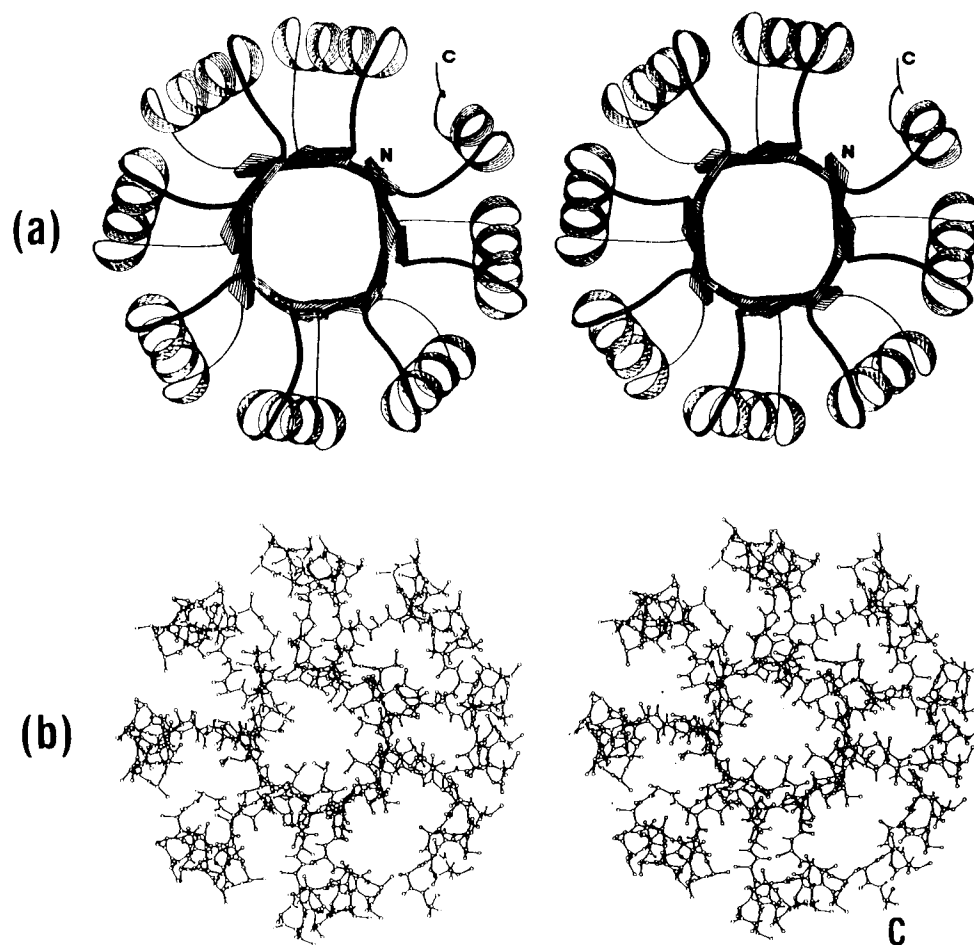


Fig. 5. Stereoscopic drawing of the representative starting conformation, before energy minimization, for the  $B_{II}$  type structure, i.e., the left-tilted, left-handed crossover  $(\alpha/\beta)_8$  barrel structure: (a) the ribbon drawing, and (b) the ball and stick drawing, in which only heavy atoms and the amide hydrogens are shown. The

ball and stick drawing is viewed along the axis of the central  $\beta$ -barrel, but the ribbon drawing is viewed opposite to that direction so that the arrows of all the  $\beta$ -strands are pointed to the viewer.

starting structures in each of these six sets, the one that had the lowest energy was chosen to represent that type of  $\alpha/\beta$  barrel for structural illustration. The stereo drawings of such six representatives are given in Figure 5–10, representing the left-tilted and left-handed crossover (Fig. 5), left-tilted and right-handed crossover (Fig. 6), nontilted and left-handed crossover (Fig. 7), nontilted and right-handed crossover (Fig. 8), right-tilted and left-handed crossover (Fig. 9), and right-tilted and right-handed crossover (Fig. 10)  $(\alpha/\beta)_8$  barrels, respectively.

It should be pointed out that there is no guarantee that the lowest energy sequentially connected structure generated by the procedure must be the lowest energy structure after energy minimization. Quite often, however, a sequentially connected structure with a large conformational energy breaks up in the energy minimization step.<sup>20</sup> From this point of view,

therefore, the above screening procedure did effectively help us in finding good starting conformations by promptly excluding many bad ones. Actually, an extensive preliminary calculation has been carried out, indicating that for most cases here the lower the energy of the starting structure, the lower the energy the final structure would reach by energy minimization. Especially, for a given type of  $\alpha/\beta$  structure selecting different starting points might get different energy-minimized values, but it would never change the basic conclusions derived from the 10 starting structures as will be shown later. The goal of the current research is to demonstrate the relative stability among the six types of  $\alpha/\beta$  structures in terms of some rational procedures, but not to search the real unique minimum energy through rigorous mathematical procedures that is technically impossible to date even for a much simpler structure.

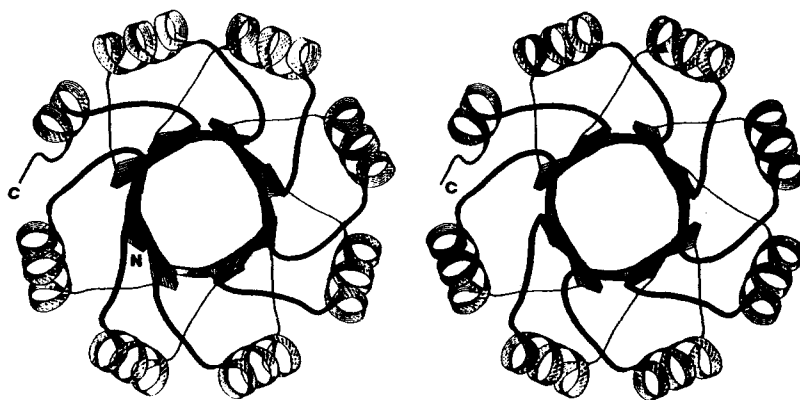


Fig. 6. Stereoscopic ribbon drawing of the representative starting conformation, before energy minimization, for the  $B_L$  type structure, i.e., the left-tilted, right-handed crossover  $(\alpha/\beta)_8$  barrel structure. Viewed opposite to the direction of the axis of the the central  $\beta$ -barrel so that the arrows of all the  $\beta$ -strands are pointed to the viewer.

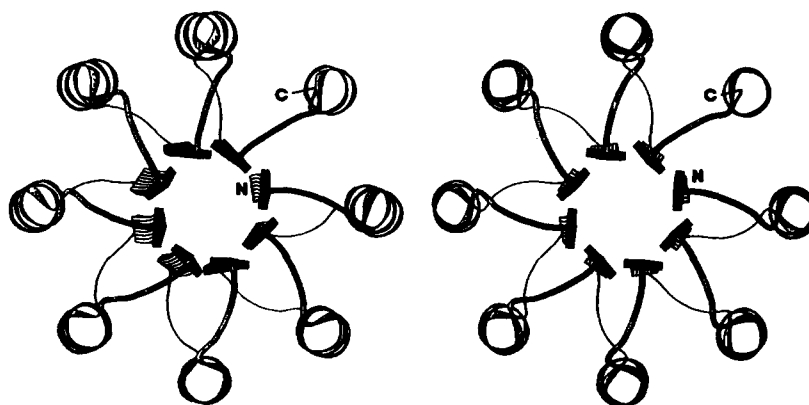


Fig. 7. Stereoscopic ribbon drawing of the representative starting conformation, before energy minimization, for the  $B_N$  type structure, i.e., the nontilted, left-handed crossover  $(\alpha/\beta)_8$  barrel structure. See the legend to Figure 6 for further explanation.

## ENERGY MINIMIZATION

The conformations obtained in the previous section were used as starting points for energy minimization. The energy was computed with the updated version (ECEPP/2) of the ECEPP algorithm (Empirical Conformational Energy Program for Peptides).<sup>24,25</sup> The total energy is the sum of the electrostatic, nonbonded, hydrogen bond, and torsional energies. A general unconstrained optimizing algorithm was used for minimization.<sup>26</sup> The computations were carried out on an IBM 3090/200 computer at Upjohn. The standard conventions for the nomenclature of peptide conformations have been followed.<sup>27</sup>

For each of the 60 starting structures sifted out by the screening procedure as described in the previous section, energy minimization was carried out according to the following steps (the resultant conformation obtained from each step was used as the starting point for the next step).

1. All backbone dihedral angles were kept fixed, and the energy was minimized with respect to all the side chain dihedral angles only, i.e., 228 variables, in order to eliminate side chain atomic overlaps.

2. All the coordinates of the atoms in the  $\beta_s$  segments were *quasifixed*, and the energy was minimized with respect to the backbone dihedral angles of all loop ( $l_p$ ) and helix ( $\alpha_h$ ) segments, then followed by step 1. In order to quasifix the coordinates of the atoms in the  $\beta_s$  segments, the following measures were adopted. (a) All the dihedral angles in the  $\beta_s$  segments were fixed. (b) A penalty function was imposed as given below

$$P_t = \sum_{m=1}^8 \{(\mathbf{r}_{mi} - \mathbf{r}_{mi}^0)^2 + (\mathbf{r}_{mj} - \mathbf{r}_{mj}^0)^2 + (\mathbf{r}_{mk} - \mathbf{r}_{mk}^0)^2\} \quad (3)$$

where  $\mathbf{r}_{mi}$ ,  $\mathbf{r}_{mj}$ , and  $\mathbf{r}_{mk}$  are the coordinates of the  $C^\alpha$  atoms in the  $i$ -,  $j$ -, and  $k$ th residues of the  $m$ th strand, respectively, with  $\mathbf{r}^0$  standing for the atomic coordinate before the current minimization, and  $\mathbf{r}$  for that obtained after minimization. For a  $\beta$ -strand

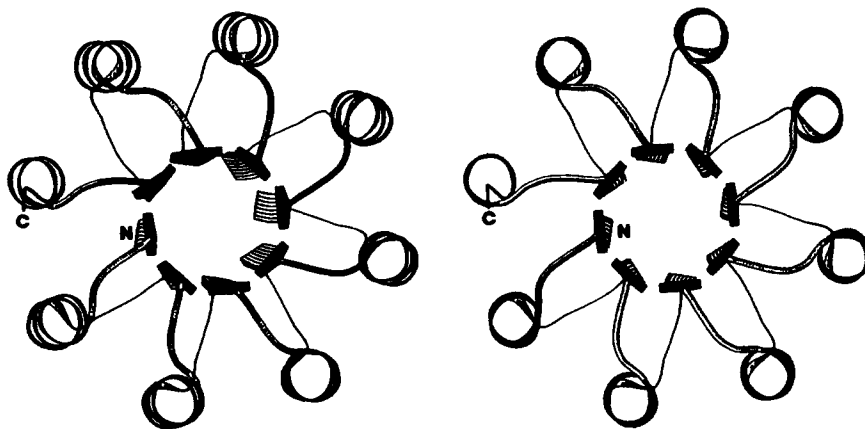


Fig. 8. Stereoscopic ribbon drawing of the representative starting conformation, before energy minimization, for the  $B_n$  type structure, i.e., the nontilted, right-handed crossover  $(\alpha/\beta)_8$  barrel structure. See the legend to Figure 6 for further explanation.

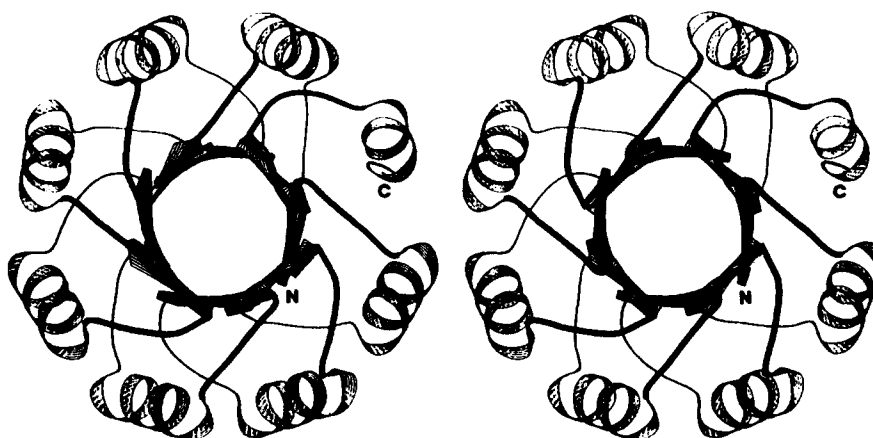


Fig. 9. Stereoscopic ribbon drawing of the representative starting conformation, before energy minimization, for the  $B_l$  type structure, i.e., the right-tilted, left-handed crossover  $(\alpha/\beta)_8$  barrel structure. See the legend to Figure 6 for further explanation.

with six residues,  $i, j$ , and  $k$  can be assigned with any three numbers of 1, 2, . . . , 6. In these calculations,  $(i, j, k)$  was assigned as (2, 3, 5). Thus, rather than minimizing the total energy  $E$  of a chain, the minimization was carried out for the pseudoenergy as given by

$$\Lambda = E + \lambda P_f \quad (4)$$

where  $\lambda$  is the weight factor, which can be assigned by any value and whose role is to enlarge the effect of the penalty function  $P_f$ . Therefore, the greater the weight factor  $\lambda$  is, the stronger the corresponding atoms are held fixed, resulting in the better fixation of the coordinates of the atoms in the  $\beta_s$  segments. The weight factor was assigned as  $\lambda = 200$  at this step.

The purpose of combining such a quasi-fixing measure for the coordinates of the atoms in the  $\beta_s$  segments is to reduce the possibility that the hydro-

gen bonds between  $\beta$ -strands might be ruptured during the energy minimization of early stage due to possible atomic overlaps.

3. All the coordinates of the atoms in the  $\beta_s$  segments were quasifixed by assigning the weight factor  $\lambda = 50$  in Eq. (4), and then the pseudoenergy  $\Lambda$  was minimized with respect to the backbone dihedral angles of all loop ( $l_p$ ) segments, then followed by step 1.

4. Release the quasifixed constraint on the  $\beta_s$  segments, i.e., assign  $\lambda = 0$ . The energy was further minimized only with respect to the backbone dihedral angles of the 8  $\beta$ -strands ( $\beta_s$  segments), and all the other dihedral angles were fixed. The energy minimization of this step was actually carried out for the inner core of the  $\alpha/\beta$  structure. Again, the energy minimization of this step was completed by repeating step 1.

5. Finally, the energy was minimized with respect

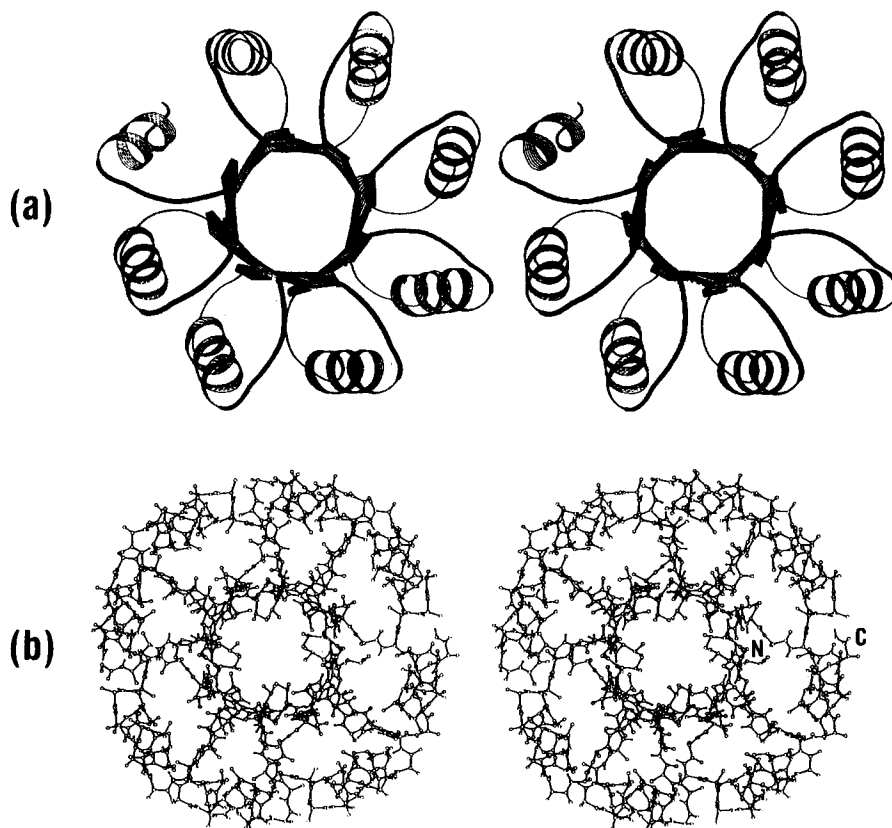


Fig. 10. Stereoscopic drawing of the representative starting conformation, before energy minimization, for the  $B_{rr}$  type structure, i.e., the right-tilted, right-handed crossover  $(\alpha/\beta)_8$  barrel structure: (a) the ribbon drawing, and (b) the ball and stick drawing, in which only heavy atoms and the amide hydrogens are shown. See the legend to Figure 5 for further explanation.

to all dihedral angles of the entire chain, i.e., 840 variables.

In the process of energy minimization, the central barrel of the  $(\alpha/\beta)_8$  structure was monitored to see whether it was broken or not. Such a monitor was promptly realized by showing the distances between the atoms involved in forming the hydrogen bond  $C' = O \cdots H - N$  holding two neighboring strands, i.e., the distance  $r_{OH}$  between atoms O and H, and the distance  $r_{C'N}$  between atoms C' and N. These distances in an idealized 8-stranded parallel  $\beta$ -barrel are<sup>16</sup>

$$r_{OH} = 2.0 \text{ \AA}$$

$$r_{C'N} = \sqrt{(2.0 \sin 20^\circ)^2 + [2.0 \cos 20^\circ + 2.23 \cos(\frac{180^\circ}{8})]^2} \text{ \AA} \quad (5)$$

Although there is no strict cutoff about the range of hydrogen bonding, it is generally believed that the stretching limitation for a hydrogen bond is within 0.5 Å. Therefore, a H-bond is considered to be intact or exist when (1)  $1.5 \text{ \AA} < r_{OH} < 2.5 \text{ \AA}$ , and (2)  $3.5 \text{ \AA} < r_{C'N} < 4.5 \text{ \AA}$ ; otherwise it is highly deformed or broken. A  $\beta$ -barrel is considered to be broken if all

H-bonds between any two of its neighboring strands are broken.

## RESULTS AND DISCUSSION

For each set of the 10 structures belonging to a same type of  $\alpha/\beta$  structure, the one whose energy was the lowest after energy minimization was chosen as a representative of that type structure for the following discussion. The data listed in Tables I–IV were also derived from these representative structures.

After energy minimizations, the central parallel  $\beta$ -barrel remained unbroken only in the  $B_{ll}$  or  $B_{rr}$  structure, i.e., the left-tilted, left-handed crossover  $(\alpha/\beta)_8$  structure or the right-tilted, right-handed crossover  $(\alpha/\beta)_8$  structure, but it was broken in all the other types of  $(\alpha/\beta)_8$  structures, as shown in Table I. This indicates that it is energetically unfavorable for a parallel  $\beta$ -barrel to dwell as an inner core in the  $B_{lr}$ ,  $B_{nl}$ ,  $B_{nr}$ , and  $B_{rl}$  type structures. The stereo drawings for the energy-minimized  $B_{ll}$  and  $B_{rr}$  structures, which each contains an unbroken central  $\beta$ -barrel, are given in Figures 11 and 12, respec-



TABLE I. The Outcome of Minimizing the Energies of Six Types of  $(\alpha/\beta)_8$  Structures\*

Type of starting $(\alpha/\beta)_8$ structure	Energy (kcal/mol)				General appearance of the central $\beta$ -barrel
	$E_{es}^{\ddagger}$	$E_{nb}^{\S}$	$E_{tor}^{**}$	$E_{tot}^{††}$	
$B_{ll}$	1110.1	-1242.0	45.2	-86.7	Parallel $\beta$ -barrel with 8 left-tilted and left-handed twisted strands
$B_{lr}$	—	—	—	—	Broken
$B_{nl}$	—	—	—	—	Broken
$B_{nr}$	—	—	—	—	Broken
$B_{rl}$	—	—	—	—	Broken
$B_{rr}$	1096.0	-1339.0	30.9	-212.1	Parallel $\beta$ -barrel with 8 right-tilted and right-handed twisted strands

\*Only the representative structure of each type is listed. The representative structure is the one which has the lowest minimized energy among the structures of that type, as defined in the text.

<sup>†</sup> $B_{ll}$  represents the left-tilted, left-handed crossover  $(\alpha/\beta)_8$  barrel,  $B_{lr}$  the left-tilted, right-handed crossover  $(\alpha/\beta)_8$  barrel,  $B_{nl}$  the nontilted, left-handed crossover  $(\alpha/\beta)_8$  barrel,  $B_{nr}$  the nontilted, right-handed crossover  $(\alpha/\beta)_8$  barrel,  $B_{rl}$  the right-tilted, left-handed crossover  $(\alpha/\beta)_8$  barrel, and  $B_{rr}$  the right-tilted, right-handed crossover  $(\alpha/\beta)_8$  barrel.

<sup>‡</sup>Electrostatic component of the total conformational energy.

<sup>§</sup>Nonbonded component of the total conformational energy.

<sup>\*\*</sup>Torsional component of the total conformation energy.

<sup>††</sup>Total conformational energy of the entire  $(\alpha/\beta)_8$  molecule; i.e.,  $E_{tot} = E_{es} + E_{nb} + E_{tor}$ .

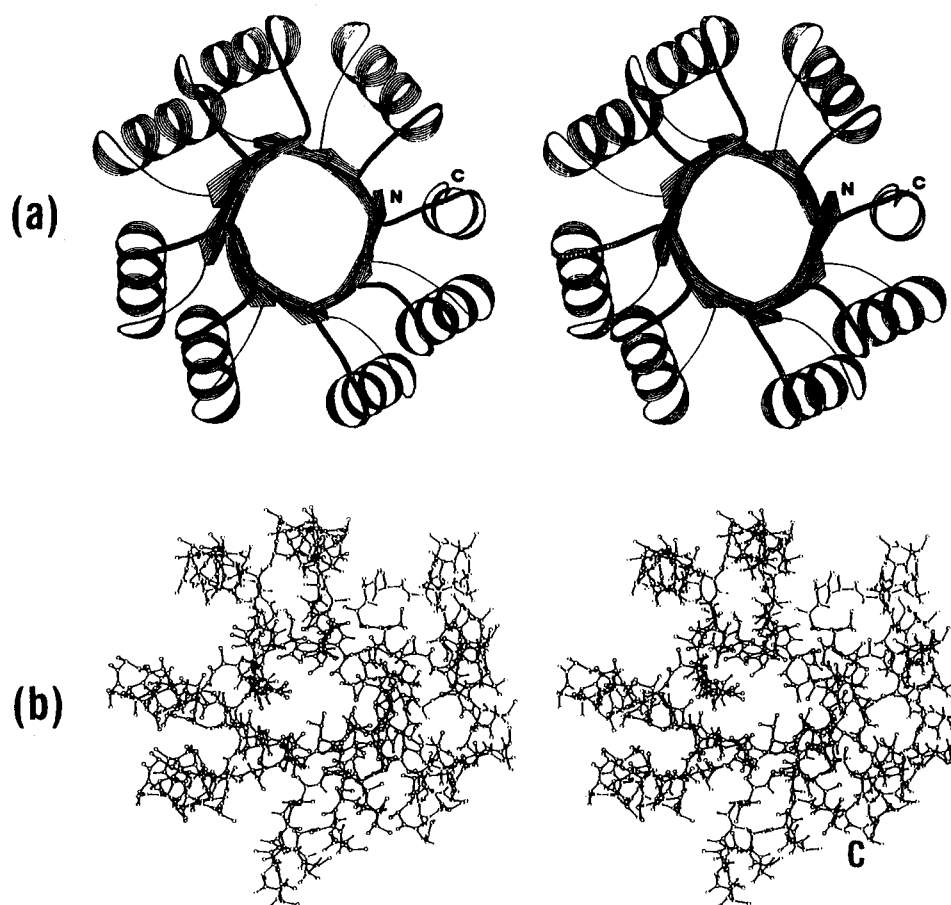


Fig. 11. Stereoscopic drawing of the energy-minimized  $B_{ll}$  structure, i.e., the left-tilted, left-handed crossover  $(\alpha/\beta)_8$  barrel: (a) the ribbon drawing, and (b) the ball and stick drawing, in which only heavy atoms and the amide hydrogens are shown. See the legend to Figure 5 for further explanation.

tively. It is also shown in Table I that the energy-minimized  $B_{rr}$  structure is 125.4 kcal/mol lower in energy than the energy-minimized  $B_{ll}$  structure,

elucidating from an energetic point of view why the observed  $\alpha/\beta$  barrels in proteins are always of right tilt and right-handed crossover connection. Energy

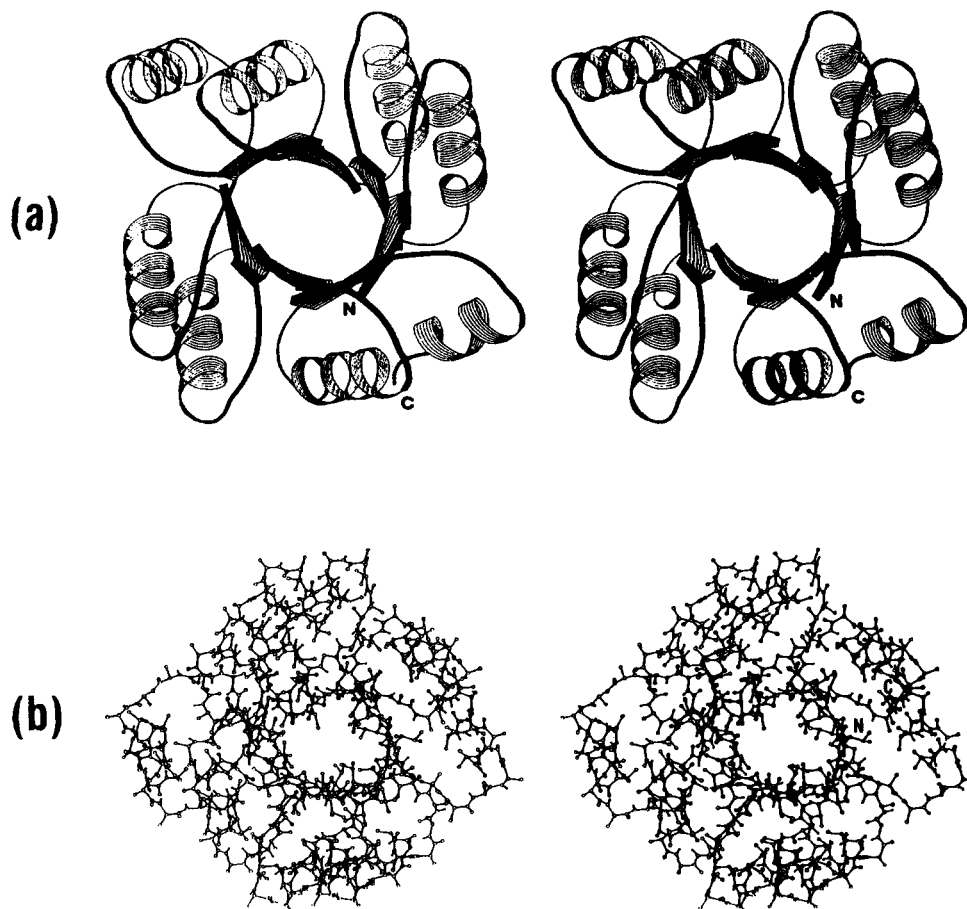


Fig. 12. Stereoscopic drawing of the energy-minimized  $B_{rr}$  structure, i.e., the right-handed, right-crossover  $(\alpha/\beta)_8$  barrel: (a) the ribbon drawing, and (b) the ball and stick drawing, in which only heavy atoms and the amide hydrogens are shown. See the legend to Figure 5 for further explanation.

in favor of the  $B_{rr}$  structure is largely contributed from the nonbonded interactions. It is interesting to see from Table I that the electrostatic energies in both  $B_{rr}$  and  $B_{ll}$  structures are positive. This can be understood because the 8 peripheral  $\alpha$ -helices around the central parallel  $\beta$ -barrel are oriented in a manner closer to a parallel than an antiparallel arrangement (Figs. 11–12). However, a parallel arrangement of neighboring  $\alpha$ -helices is unfavorable in electrostatic interactions between the helices caused by the large dipole moments of the  $\alpha$ -helices.<sup>28–30</sup> Therefore, the positive electrostatic interaction energy is a common feature for the  $\alpha/\beta$  barrel structures. More discussion about energies contributed from different segments of the  $\alpha/\beta$  structures will be given later.

Before energy minimization the six types of  $(\alpha/\beta)_8$  structures each contains an idealized parallel  $\beta$ -barrel (Figs. 2–4), in which there are 5 H-bonds between its two neighboring  $\beta$ -strands, for a total of  $5 \times 8 = 40$  H-bonds.<sup>16</sup> After energy minimizations for the  $B_{lr}$ ,  $B_{nl}$ ,  $B_{nr}$ , and  $B_{rl}$  type structures, however, their central  $\beta$ -barrels were all broken as reflected

by the fact that the H-bonds in at least one pair of neighboring  $\beta$ -strands were totally ruptured for all these barrels. Only for the  $B_{ll}$  and  $B_{rr}$  structures did the energy minimization not break the H-bonds in their inner cores of barrels. For these two energy-minimized structures each of which represents its own type of the lowest energy thus found, the average length of H-bonds in each pair of  $\beta$ -neighboring strands is listed in Table II. It is seen from these values that none of them deviates more than 0.12 Å from the corresponding values of an idealized H-bond for an 8-stranded parallel  $\beta$ -barrel, indicating that the H-bonds of the central  $\beta$ -barrels in the energy-minimized  $B_{ll}$  and  $B_{rr}$  structures are quite normal. This can also be seen by the corresponding stereo drawings as given in Figures 11 and 12.

Why were the  $\beta$ -barrels in  $B_{lr}$ ,  $B_{nl}$ ,  $B_{nr}$ , and  $B_{rl}$  type structures broken after energy minimization? Let us consider the case of the  $B_{nl}$  and  $B_{nr}$  type structures first. The  $\beta$ -barrel contained in  $B_{nl}$  or  $B_{nr}$  type structure is a non-tilted one (Fig. 3). It has been demonstrated<sup>16</sup> that given the same length of H-bonds between  $\beta$ -strands, a nontilted  $\beta$ -barrel has a

**TABLE II. The Average Distances Between Atoms Involved in Forming C' = O...H-N Hydrogen Bonds Between Two Neighboring  $\beta$ -Strands in the Energy-Minimized  $B_{11}$  and  $B_{rr}$  Structures, Respectively**

Pair numbering two neighboring $\beta$ -strands	The average atomic distances in the 5 H-bonds between neighboring strands (Å)			
	$B_{11}$		$B_{rr}$	
	$\langle r_{OH} \rangle^*$	$\langle r_{CN} \rangle^\dagger$	$\langle r_{OH} \rangle^*$	$\langle r_{CN} \rangle^\dagger$
1-2	2.10	4.10	1.30	3.30
2-3	1.95	3.91	2.12	4.06
3-4	2.06	4.12	2.06	4.11
4-5	1.94	3.86	1.99	3.92
5-6	2.01	4.08	1.92	4.01
6-7	1.91	3.88	2.08	4.11
7-8	2.02	4.07	1.95	4.02
8-1	1.99	3.91	2.01	4.02

\* $r_{OH}$  = 2.00 Å in an idealized H-bond for the 8-stranded parallel  $\beta$ -barrel.<sup>16</sup>

† $r_{CN}$  = 3.99 Å in an idealized H-bond for the 8-stranded parallel  $\beta$ -barrel.<sup>16</sup>

smaller radius than the corresponding tilted one. Consequently, there is relatively less room for a nontilted  $\beta$ -barrel to accommodate the internal side chains, suggesting that a conformational change from a nontilted  $\beta$ -barrel to a tilted one would ease the repulsion among the crowded internal side chains. However, such a conformational change must first break the nontilted  $\beta$ -barrel. And once it was broken, the tilted  $\beta$ -barrel was hardly reassembled driven by energy minimization. That is why no unbroken  $\beta$ -barrel remained after energy minimization for the  $B_{n1}$  and  $B_{nr}$  type structures. Now let us consider the case of the  $B_{1r}$  and  $B_{r1}$  type structures. It is apparent from Figures 2 and 4 that the distances for crossover connections between two neighboring  $\beta$ -strands of the central barrel in these two type structures are longer than those in the  $B_{11}$  and  $B_{rr}$  type structures. In studying  $\beta\alpha\beta$  structures, Sternberg and Thornton<sup>31</sup> pointed out that if two  $\beta$ -strands are connected in a shorter and geometrically simpler manner, then the connected structure is likely to be less strained. In other words, in proteins the topology corresponding to the short connection is overwhelmingly preferred (even though the polypeptide backbone itself does not necessarily follow the shortest path). This effect is particularly important whenever the connecting oligopeptide links between the  $\alpha$ -helix and the  $\beta$ -strands are short such as in the current case, and it has been borne out through energy calculations.<sup>6</sup> To change these strained crossover connections which are energetically extremely unfavorable, the central  $\beta$ -barrel must undergo a change from its original left or right tilt toward right or left tilt, respectively. Such a process would of course result in an irreversible breakage of the central  $\beta$ -barrel too. That is why no unbroken  $\beta$ -barrel remained after energy minimization for the  $B_{1r}$  and  $B_{r1}$  type structures either. Consequently, it is not difficult to understand why after energy minimization the  $\beta$ -barrels only in  $B_{11}$  and

$B_{rr}$  structures survived without being broken. However, it is not so clear why the energy-minimized structure  $B_{rr}$  is more stable than the energy-minimized  $B_{11}$  structure, as reflected by the much lower conformational energy. In order to reveal this, a detailed analysis in both geometry and energetics for these two structures is needed, and will be presented below.

The geometric parameters characterizing the central  $\beta$ -barrels in the energy-minimized  $B_{11}$  and  $B_{rr}$  structures are listed in Table III. As expected, all the strands in the  $B_{11}$  structure are left-tilted, with an average tilted value  $\langle \theta \rangle = 30^\circ$ . Conversely, all the strands in the  $B_{rr}$  structure are right-tilted, with an average tilted value  $\langle \theta \rangle = -32^\circ$ , which is very close to the tilted angle of  $-36^\circ$  as observed by Banner et al.<sup>1</sup> for the  $(\alpha/\beta)_8$  barrel in the triose phosphate isomerase (TIM). Besides, all the strands in the  $B_{11}$  structure are left-handed twisted, and those in the  $B_{rr}$  structure are strongly right-handed twisted, as reflected by the fact that the average value of  $\langle \delta \rangle$  for the former is  $-20^\circ$  and that for the latter is  $44^\circ$ . The strong right-handed twist of the  $\beta$ -strands in a  $\beta$ -barrel is a common feature of all observed  $\beta$ -barrels in proteins,<sup>2,5,7,9,10,32,33</sup> and its implication in stabilizing the right-tilted, right-handed crossover  $\alpha/\beta$  barrel will be further discussed later.

It is interesting to note the data of  $d_r$  as listed in the seventh column of Table III. These data, each of which represents the radial distance of a strand to the central axis of the barrel, actually reflect the shape of the cross section at the middle of the central  $\beta$ -barrel (Fig. 13). Before energy minimization, the central  $\beta$ -barrel is an idealized one, i.e., a regularly cylinder-like structure with  $d_r = 7.3$  Å for all the strands.<sup>16</sup> Obviously, the cross section of such a barrel is a circle with a radius  $r = 7.3$  Å (Fig. 13a). After energy minimization, however, its shape was changed from a circle to an ellipse (Fig. 13b). This is

**TABLE III. Geometric Parameters Characterizing the Central  $\beta$ -Barrels in the Energy-Minimized  $B_{11}$  and  $B_{rr}$  Structures**

	$B_{11}$			$B_{rr}$		
	$\langle \delta \rangle^*$ (deg)	$\theta^+$ (deg)	$d_r^{c\ddagger}$ (Å)	$\langle \delta \rangle^*$ (deg)	$\theta^+$ (deg)	$d_r^{c\ddagger}$ (Å)
Strand						
1	-14.8	31.5	7.3	49.9	-36.7	7.9
2	-23.4	30.9	7.5	51.0	-31.1	6.3
3	-18.1	29.1	6.9	36.0	-22.5	6.4
4	-25.5	30.0	7.0	42.0	-32.6	8.3
5	-16.3	30.9	7.2	41.4	-38.3	7.7
6	-25.1	33.1	7.5	45.0	-32.2	6.4
7	-17.4	29.4	6.9	36.8	-25.2	6.5
8	-21.9	29.4	7.1	45.6	-34.0	8.1
Average of 8 strands	-20.3	30.4	7.2	43.5	-31.6	7.2
$\langle \Omega_0 \rangle^{\S}$ (deg)		22			-30	
$\Omega_{\alpha\beta}^{++}$ (deg)		$180 \pm 20^\circ$			$180 \pm 18^\circ$	

\*The average twist of  $\beta$ -strand. See Chou et al.<sup>38</sup> for the definition of  $\delta$ . The right-handed twist, left-handed twist, and nontwist correspond to  $\delta > 0$ ,  $\delta < 0$ , and  $\delta = 0$ , respectively.

<sup>†</sup>The tilted angle of a constituent  $\beta$ -strand to the central axis of a barrel.<sup>16</sup> The right-tilted, left-tilted, and nontilted  $\beta$ -strands correspond to  $\theta < 0$ ,  $\theta > 0$ , and  $\theta = 0$ , respectively.

<sup>‡</sup>The radial distance from the central axis of a  $\beta$ -barrel to each of its strands. The data of  $d_r$  can be used to describe the shape of cross section of a  $\beta$ -barrel, as shown in Figure 13.

<sup>§</sup>The average orientational angle<sup>22</sup> between two neighboring  $\alpha$ -helices.

<sup>++</sup>The packing angle<sup>23</sup> of an  $\alpha$ -helix against the  $\beta$ -sheet formed by the two strands connected by the helix via a crossover.

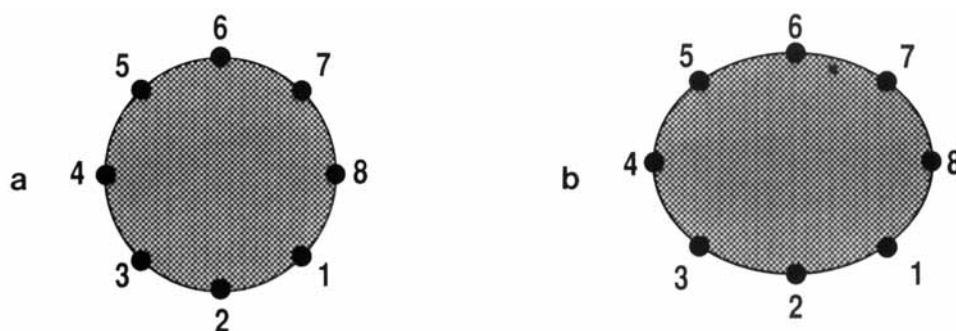


Fig. 13. The cross section of (a) the idealized 8-stranded parallel  $\beta$ -barrel in which the radial distances from the axis of the barrel to all the constituent strands are the same, i.e.,  $d_r = 7.3$  Å,<sup>16</sup> and (b) the central  $\beta$ -barrel of the energy-minimized  $B_{rr}$  structure in which the values of  $d_r$  are different for the 8 constituent strands as shown in Table III. The shape of the cross section in (a) is a circle, but that in (b) is an ellipse.

an encouraging sign because the elliptical cross section is a common geometric feature for observed  $\beta$ -barrels in proteins.<sup>3,5,33,34</sup> Therefore, after energy minimization the  $\beta$ -barrel in the  $B_{rr}$  structure is more close to the observed  $\beta$ -barrels. As a further demonstration, a skeleton stereo drawing to show the fitness of backbone atoms between the central  $\beta$ -barrel of the energy-minimized  $B_{rr}$  structure and the parallel 8-stranded  $\beta$ -barrel in TIM is given in Figure 14, where the computed  $\beta$ -barrel was drawn in red and the observed  $\beta$ -barrel was drawn in blue. The atomic coordinates for TIM were obtained from the Brookhaven Protein Data Bank, based on the work by Banner et al.<sup>1</sup> In comparison with the previous stereo drawing showing the fitness between the corresponding idealized  $\beta$ -barrel and the  $\beta$ -

barrel in TIM (see Fig. 9a of ref. 16), it can be seen that the current fitting was improved. The better fitting is also indicated by the smaller value of the root-mean-square (RMS) fit, which is 1.4 Å now vs. 1.6 Å of the previous value.<sup>16</sup> It should be pointed out that such a change in shape of the cross section from a circle to an ellipse did not occur when minimizing the energy of an idealized  $\beta$ -barrel consisting of sequentially separate  $\beta$ -strands (see Fig. 2 of ref. 17). Therefore, the elliptical cross section as generally occurs in observed  $\beta$ -barrels was caused by the effect of the connecting segments between the  $\beta$ -strands.

The arrangements of the 8  $\alpha$ -helices at the periphery of the energy-minimized  $B_{11}$  and  $B_{rr}$  structures are as follows. The average orientational angle<sup>22,35</sup>

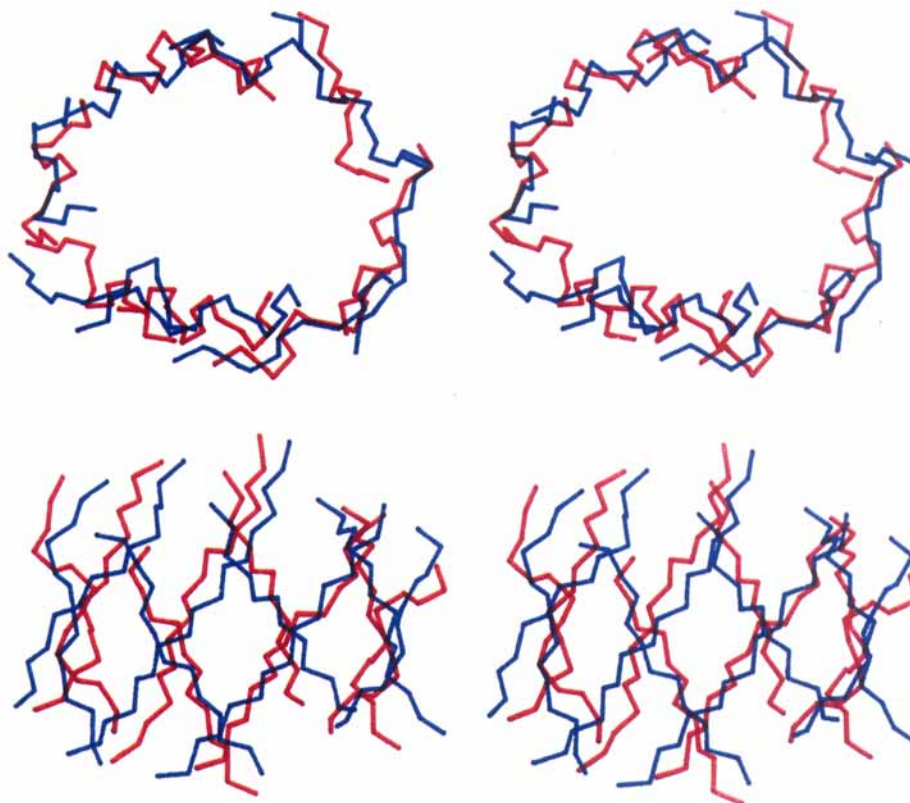


Fig. 14. Stereoscopic skeleton drawing to show the fitness between the central parallel  $\beta$ -barrel of the energy-minimized  $B_{II}$  structure and the observed parallel  $\beta$ -barrel in TIM (RMS deviation = 1.4 Å): (a) viewed along the axis of  $\beta$ -barrel, and (b) viewed from the side of  $\beta$ -barrel. Only the  $\beta$ -barrel backbone atoms N, C $^{\alpha}$ , and C' were used for the least-squares fitting.<sup>16,33</sup> The observed  $\beta$ -barrel was drawn in blue and the computed  $\beta$ -barrel drawn in red.

$\langle \Omega_0 \rangle$  between two neighboring helices is  $22^\circ$  for the  $B_{II}$  structure and  $-30^\circ$  for the  $B_{rr}$  structure; i.e., the 8  $\alpha$ -helices in the former follow a left-handed spiral around the barrel axis and those in the latter follow a right-handed spiral around the barrel axis. The packing angle<sup>23</sup>  $\Omega_{\alpha\beta}$  of an  $\alpha$ -helix against the  $\beta$ -sheet formed by the two  $\beta$ -strands it connects is  $180^\circ \pm 20^\circ$  for the  $B_{II}$  structure and  $180^\circ \pm 18^\circ$  for the  $B_{rr}$  structure, i.e., the axes of the  $\alpha$ -helices are approximately parallel to the  $\beta$ -strands. Both of these features regarding the arrangement of  $\alpha$ -helices as occurred in the low-energy  $B_{rr}$  structure are usual in the observed  $\alpha/\beta$  barrels.<sup>2,3,5,11</sup>

In order to compare and analyze the energetics contributed from different segments of the  $(\alpha/\beta)_8$  barrel structure and their interactions, let us separate the total conformational energy  $E_{tot}$  of the entire  $(\alpha/\beta)_8$  molecule into the terms as defined below:

$E_{intra}^{\alpha}$  = Sum of the energies of the 8 individual constituent  $\alpha$ -helices ( $\alpha_{hs}$ )

$E_{inter}^{\alpha}$  = Total intersegment energy among the 8  $\alpha$ -helices

$$E_{tot}^{\alpha} = E_{intra}^{\alpha} + E_{inter}^{\alpha}$$

$E_{intra}^{\beta}$  = Sum of the energies of the 8 individual constituent  $\beta$ -strands ( $\beta_{ss}$ )

$E_{inter}^{\beta}$  = Total intersegment energy among the 8  $\beta$ -strands

$$E_{tot}^{\beta} = E_{intra}^{\beta} + E_{inter}^{\beta}$$

$E_{inter}^{\alpha/\beta}$  = Total intersheet energy between  $\alpha$ -helices and  $\beta$ -strands, i.e., the interaction energy between the outer helices and inner core of barrel (6)

$$E_{tot}^{\alpha/\beta} = E_{tot}^{\alpha} + E_{tot}^{\beta} + E_{inter}^{\alpha/\beta}$$

$E_{intra}^{loop}$  = Sum of the energies of the 15 individual loops ( $\ell_{ps}$ )

$E_{inter}^{loop}$  = Total intersegment energy among the 15 loops

$$E_{tot}^{loop} = E_{intra}^{loop} + E_{inter}^{loop}$$

$\tilde{E}_{tot}^{loop} = E_{tot}^{loop} + \epsilon$ , where  $\epsilon$  is the interaction energy between the loops and all the other part of the molecule

$\tilde{E}_{tot}^{loop}$  in the above equation is called associated loop

TABLE IV. Various Energetic Terms Characterizing the Energy-Minimized  $B_{11}$  and  $B_{rr}$  Structures\*

Type of ( $\alpha/\beta$ ) <sub>8</sub> barrel	Energy of $\alpha_h$ set (kcal/mol)			Energy of $\beta_s$ set (kcal/mol)			Energy of $\alpha_h/\beta_s$ set (kcal/mol)		Loop-related energy (kcal/mol)					Energy of entire molecule
	$E_{intra}^{\alpha}$	$E_{inter}^{\alpha}$	$E_{tot}^{\alpha}$	$E_{intra}^{\beta}$	$E_{inter}^{\beta}$	$E_{tot}^{\beta}$	$E_{intra}^{\alpha/\beta}$	$E_{tot}^{\alpha/\beta}$	$E_{loop}^{intra}$	$E_{loop}^{inter}$	$E_{loop}^{tot}$	$\epsilon$	$\bar{E}_{tot}^{loop}$	$E_{tot}$
$B_{11}$	-45.1	-24.2	-69.3	224.8	-215.5	9.3	-59.9	-119.9	393.4	-45.0	348.4	-315.2	33.2	-86.7
$B_{rr}$	-45.0	-26.1	-71.1	196.2	-201.2	-4.0	-50.2	-137.1	286.5	-14.4	279.1	-247.1	-75.0	-91.9

\*See Eq. (6) for the definition of each of the energetic terms.

energy, which is defined by augmenting  $E_{tot}^{loop}$  to incorporate  $\epsilon$ , the interaction term between the loop segments and the other part of the ( $\alpha/\beta$ )<sub>8</sub> molecule,<sup>20,21</sup> and hence represents the total energy associated with the loops. From Eq. (6) we obviously have

$$E_{tot} = \bar{E}_{tot}^{loop} + E_{tot}^{\alpha/\beta} \quad (7)$$

Listed in Table IV are the values of the energetic terms as defined in Eq. (6) for the energy-minimized  $B_{11}$  and  $B_{rr}$  structures, respectively. As we can see, the total conformational energy in the  $B_{rr}$  structure is 125.4 kcal/mol lower than that in the  $B_{11}$  structure. From Eq. (7) and Table IV we can further see that of such an energy gap 108.2 kcal/mol is from  $\bar{E}_{tot}^{loop}$  and only 17.2 kcal/mol is from  $E_{tot}^{\alpha/\beta}$ . Therefore, it is the associated loop energy  $\bar{E}_{tot}^{loop}$  which plays the major role in favor of the right-tilted and right-handed crossover ( $\alpha/\beta$ )<sub>8</sub> structure. This is because the intraloop energy  $E_{intra}^{loop}$  and the interaction  $\epsilon$  between the loop segments and the other part of the molecule are much more favorable to  $B_{rr}$  than  $B_{11}$ . Moreover, the interhelix energy  $E_{inter}^{\alpha}$  and intra-strand energy  $E_{intra}^{\beta}$  are favorable in making  $E_{tot}^{\alpha/\beta}$  have lower energy in  $B_{rr}$  than in  $B_{11}$ . This is completely consistent with the computed results on the packing of  $\alpha$ -helices and the twist of  $\beta$ -strands. Recall that the average orientational angle  $\langle \Omega_0 \rangle$  between two neighboring helices in the  $B_{11}$  structure is 22° and that in the  $B_{rr}$  structure is -30° (Table III). It was indicated in the previous paper<sup>35</sup> that the packing between two  $\alpha$ -helices has a lower energy at the arrangement with the orientational angle  $\Omega_0$  around -30° than 22°. That is why the interhelix energy  $E_{inter}^{\alpha}$  is lower in the  $B_{rr}$  structure than in the  $B_{11}$  structure. On the other hand, a  $\beta$ -strand generally has lower energy when it is right-handed twisted than left-handed twisted.<sup>36-38</sup> In harmonizing with the right-tilted and right-handed crossover geometry, all the  $\beta$ -strands in the  $B_{rr}$  structure are in the lower energy form of right-handed twisting, but in the  $B_{11}$  structure the presence of a left-tilted barrel and left-handed crossover connection forces the  $\beta$ -strands into the energetically less favorable left-twisted form (Table III). That is why the intra-strand energy  $E_{intra}^{\beta}$  is lower in the  $B_{rr}$  structure than in the  $B_{11}$  structure.

Therefore, the calculated energy in favor of the

right-tilted, right-handed crossover  $\alpha/\beta$  barrel is correlated with the fact that right-handed twisted  $\beta$ -sheets are more stable than left-handed twisted or non-twisted  $\beta$ -sheets.<sup>36-38</sup> Similar correlation<sup>6,20</sup> has also been found in  $\beta\alpha\beta$  and Rossmann fold structures. The highly consistent results derived from different types of structures indicate that although the energetic calculations in this paper were performed on a particular sequence of polypeptide, the applicability of the derived conclusions to proteins is general.

## CONCLUSIONS

Six different types of  $\alpha/\beta$  barrels, classified according to the tiltedness of the  $\beta$ -strands and the handedness of crossover connection between two neighboring  $\beta$ -strands, were generated and energy-minimized. After energy minimizations, only in the right-tilted and right-handed crossover connection  $\alpha/\beta$  structure or in the left-tilted and left-handed crossover connection  $\alpha/\beta$  structure did the central  $\beta$ -barrel remain unbroken. The central  $\beta$ -barrels in all the other four types of  $\alpha/\beta$  structures were destroyed after energy minimizations, as reflected by the fact that the original arrangement of hydrogen bonds of cylindrical pattern in these structures was substantially damaged so that the  $\beta$ -strands were no longer held to have a general shape of a barrel. The  $\beta$ -barrel contained in the nontilted and either right-handed or left-handed crossover  $\alpha/\beta$  structure is unstable because its radius is smaller than those in the corresponding tilted  $\alpha/\beta$  structures, suggesting that a conformational change from a nontilted  $\beta$ -barrel to a tilted one would ease the repulsion among the crowded internal side chains.<sup>16</sup> However, driven by energy minimization rather than nature, such a conformational change must end with an irreversible breakage of the barrel. The  $\beta$ -barrels in the left-tilted and right-handed crossover  $\alpha/\beta$  structure and in the right-tilted and left-handed crossover  $\alpha/\beta$  structure are also unstable because the distances for the crossover connections between neighboring  $\beta$ -strands of the central barrels in these two structures are longer than those of the others, representing more strained<sup>31</sup> and less energetically favorable.<sup>6</sup> However, between the two  $\alpha/\beta$  structures whose central  $\beta$ -barrels remained unbroken after energy minimizations, the right-tilted and right-handed cross-

over  $\alpha/\beta$  structure ( $B_{rr}$ ) is 125 kcal/mol lower in energy than the left-tilted and left-handed crossover  $\alpha/\beta$  structure ( $B_{ll}$ ). Such a large energy gap is mainly caused by the associated loop energy which plays a key role in favor of the right-tilted and right-handed crossover ( $\alpha/\beta$ )<sub>8</sub> structure, as reflected by the fact that both the intraloop energy and the interaction between the loop segments and the other part of the molecule are much more favorable in this structure ( $B_{rr}$ ) than its left-handed counterpart ( $B_{ll}$ ), as shown in Table IV. Moreover, the interhelix energy and intrastrand energy provide additional contributions in favor of the right-tilted and right-handed crossover  $\alpha/\beta$  structure ( $B_{rr}$ ).

The results presented here indicate that the right-tilted and right-handed crossover  $\alpha/\beta$  barrel structure is the energetically most stable type of structure among the six types of  $\alpha/\beta$  structures. This is fully in agreement with the observations that so far all the known  $\alpha/\beta$  barrels in proteins are right-tilted and right-handed crossover connected. Besides, all the  $\beta$ -strands in the energetically most stable ( $\alpha/\beta$ )<sub>8</sub> barrel thus found are strong right-handed twisted, which is a common feature of observed  $\beta$ -barrels in proteins.<sup>2,5,7,9,10,32,33</sup> The value of root-mean-square fits between the computed parallel  $\beta$ -barrel and the observed 8-stranded parallel  $\beta$ -barrel in TIM further indicates that there is a better fitting after energy minimization than before energy minimization. All these results support the principle that it is possible to account for the main features of frequently occurring folding arrangements in proteins in terms of conformational energy calculations even for very complicated structures such as ( $\alpha/\beta$ )<sub>8</sub> barrels.

## ACKNOWLEDGMENTS

We are greatly indebted to Dr. Douglas C. Rohrer for his kind help in drawing the stereo ribbon drawings<sup>39</sup> as given in Figures 5–12. Valuable discussions with Dr. Gerald M. Maggiora and Dr. Bor-yue Mao are also gratefully acknowledged.

## REFERENCES

- Banner, D. W., Bloomer, A. C., Petsko, G. A., Philips, D. C., Wilson, I. A. Atomic coordinates for triose phosphate isomerase from chicken muscle. *Biochem. Biophys. Res. Commun.* 72:146–155, 1976.
- Lesk, A. M., Brändén, C.-I., Chothia, C. Structural principles of  $\alpha/\beta$  barrels proteins: The packing of the interior of the sheet. *Proteins: Struct. Funct. Genet.* 5:139–148, 1989.
- Farber G. K., Petsko, G. A. "The evolution of  $\alpha/\beta$  barrel enzymes", *Trends in Biochemical Sciences* 15:228–234, 1990.
- Handel, T. De novo design of an  $\alpha/\beta$  barrel protein. *Protein Engineer.* 3:233–234, 1990.
- Richardson, J. S. The anatomy and taxonomy of protein structure. *Adv. Protein Chem.* 34:167–339, 1981.
- Chou, K.-C., Némethy, G., Pottle, M., Scheraga, H. A. Energy of stabilization of the right-handed  $\beta\alpha\beta$  crossover in proteins. *J. Mol. Biol.* 205:241–249, 1989.
- Phillips, D. C., Sternberg, M. J. E., Thornton, J. M., Wilson, J. A. An analysis of the structure of triose phosphate isomerase and its comparison with lactate dehydrogenase. *J. Mol. Biol.* 119:329–351, 1978.
- Sternberg, M. J. E., Thornton, J. M. Prediction of protein structure from amino acid sequence. *Nature (London)* 271:15–20, 1978.
- McLachlan, A. D. Gene duplications in the structural evolution of chymotrypsin. *J. Mol. Biol.* 128:49–79, 1979.
- Salemme, F. R., Weatherford, D. W. Conformational and geometrical properties of  $\beta$ -sheets in proteins: 1. parallel  $\beta$ -sheets. *J. Mol. Biol.* 146:101–117, 1981.
- Richardson, J. S., Richardson, D. C. Principles and patterns of protein conformation. In: "Prediction of Protein Structure and the Principles of Protein Conformation." Fasman, G. D. (ed.). New York & London: Plenum Press: 1989: 1–98.
- Lasters, I., Wodak, S. J., Alard, P., van Cutsem, E. Structural principles of parallel  $\beta$ -barrels in proteins. *Proc. Natl. Acad. Sci. U.S.A.* 85:3338–3342, 1988.
- Lasters, I., Wodak, S. J., Pio, F. The design of idealized  $\alpha/\beta$ -barrels: Analysis of  $\beta$ -sheets closure requirements. *Proteins: Struct. Funct. Genet.* 7:249–256, 1990.
- Luger, K., Szadkowski, H., Kirschner, K. An 8-fold  $\beta\alpha$  barrel protein with redundant folding possibilities. *Protein Engineer.* 3:249–258, 1990.
- Goraj, K., Renard, A., Martial J. A. Synthesis, purification and initial structural characterization of octarellin, a de novo polypeptide modelled on the  $\alpha/\beta$ -barrel proteins. *Protein Engineer.* 3:259–266, 1990.
- Chou, K.-C., Caracci, L., Maggiora, G. M. Conformational and geometrical properties of idealized  $\beta$ -barrels in proteins. *J. Mol. Biol.* 213:315–326, 1990.
- Chou, K.-C., Heckel, A., Némethy, G., Rumsey, S., Caracci, L., Scheraga, H. A. Energetics of the structure and chain tilting of antiparallel  $\beta$ -barrels in proteins. *Proteins: Struct. Funct. Genet.* 8:14–22, 1990.
- Lifson, S., Sander, C. Antiparallel and parallel  $\beta$ -strands differ in amino acid residue preferences. *Nature (London)* 282:109–111, 1979.
- Lifson, S., Sander, C. Composition, cooperativity and recognition in proteins. In: "Protein Folding," Jaenicke, R. (ed.). Amsterdam: Elsevier/North-Holland Biomedical Press, 1980: 289–316.
- Caracci, L., Chou, K.-C. Monte Carlo method applied in the search for low energy conformations of  $\beta\alpha\beta\alpha\beta$  structures. *Biopolymers* 30:135–150, 1990.
- Caracci, L., Chou, K.-C. Energetic approach to the folding of four  $\alpha$ -helices connected sequentially. *Protein Engineer.* 3:509–514, 1990.
- Chou, K.-C., Némethy, G., Scheraga, H. A. Energetic approach to the packing of  $\alpha$ -helices. 2. General treatment of nonequivalent and nonregular helices. *J. Am. Chem. Soc.* 106:3161–3170, 1984.
- Chou, K.-C., Némethy, G., Rumsey, S., Tuttle, R. W., Scheraga, H. A. Interactions between an  $\alpha$ -helix and a  $\beta$ -sheet. Energetics of  $\alpha/\beta$  packing in proteins. *J. Mol. Biol.* 186:591–609, 1985.
- Momany, F. A., McGuire, R. F., Burgess, A. W., Scheraga, H. A. Energy parameters in polypeptides. 7. Geometric parameters, partial atomic charges, nonbonded interactions, hydrogen bond interactions, and intrinsic torsional potentials for the naturally occurring amino acids. *J. Phys. Chem.* 79:2361–2381, 1975.
- Némethy, G., Pottle, M. S., Scheraga, H. A. Energy parameters in polypeptides. 9. Updating of geometrical parameters, nonbonded interactions, and hydrogen bond interactions for the naturally occurring amino acids. *J. Phys. Chem.* 87:1883–1887, 1983.
- Gay, D. M. Subroutines for unconstrained minimization using a model/trust-region approach. *Assoc. Comput. Mach. Trans. Math. Software* 9:503–524, 1983.
- Commission on Biochemical Nomenclature. Abbreviations and symbols for the description of the conformation of polypeptide chains. *Biochemistry* 9:3471–3479, 1970.
- Wada, A. The  $\alpha$ -helix as an electric macro-dipole. *Adv. Biophys.* 9:1–63, 1976.
- Hol, W. G. J., van Duijnen, P. T., Berendsen, H. J. C. The  $\alpha$ -helix dipole and the properties of proteins. *Nature (London)* 273:443–446, 1978.
- Sheridan, R. P., Allen, L. C. The electrostatic potential of  $\alpha$ -helix. *Biophys. Chem.* 11:133–136, 1980.
- Sternberg, M. J. E., Thornton, J. M. On the conformation

- of proteins: The handedness of the  $\beta$ -strand- $\alpha$ -helix- $\beta$ -strand unit. *J. Mol. Biol.* 105:367–382, 1976.
32. Tainer, J. A., Getzoff, D. E., Beem, K. M., Richardson, J. S., Richardson, D. C. Determination and analysis of the 2 Å structure of copper, zinc superoxide dismutase. *J. Mol. Biol.* 160:181–217, 1982.
  33. Novotný, J., Brucoleri, R. E., Newell, J. Twisted hyperboloid (*strophoid*) as a model of  $\beta$ -barrels in proteins. *J. Mol. Biol.* 177:567–573, 1984.
  34. Chothia, C., Janin, J. Relative orientation of close-packed  $\beta$ -pleated sheets in proteins. *Proc. Natl. Acad. Sci. U.S.A.* 78:4146–4150, 1981.
  35. Chou, K. C., Némethy, G., Scheraga, H. A. Energetic approach to the packing of  $\alpha$ -helices. 1. Equivalent helices. *J. Phys. Chem.* 87:2869–2881, 1983.
  36. Chothia, C. Conformation of twisted  $\beta$ -pleated sheets in proteins. *J. Mol. Biol.* 75:295–302, 1973.
  37. Chou, K.-C., Scheraga, H. A. Origin of the right-handed twist of  $\beta$ -sheets of poly(L-Val) chains. *Proc. Natl. Acad. Sci. U.S.A.* 79:7047–7051, 1982.
  38. Chou, K.-C., Némethy, G., Scheraga, H. A. Effect of amino acid composition on the twist and the relative stability of parallel and antiparallel  $\beta$ -sheets. *Biochemistry* 22:6213–6221, 1983.
  39. Priesfle, J. P. Ribbon: A stereo cartoon drawing program for proteins. *J. Appl. Crystallogr.* 21:572–576, 1988.